ChemComm

RSC Publishing

COMMUNICATION

View Article Online
View Journal | View Issue

A conical intersection model to explain aggregation induced emission in diphenyl dibenzofulvene†

Cite this: *Chem. Commun.*, 2013, **49**, 5966

Received 7th March 2013,
Accepted 13th May 2013

DOI: 10.1039/c3cc41730a

www.rsc.org/chemcomm

Quansong Li[a] and Lluís Blancafort*[b]

A conical intersection seam is behind the restriction of intramolecular rotation mechanism for aggregation induced emission in diphenyl dibenzofulvene (DPDBF). In solution, the seam is accessed through rotation around the exocyclic fulvene bond, leading to radiationless decay to the ground state. In the solid, the seam cannot be accessed because the torsion is blocked, and DPDBF becomes emissive.

Aggregation induced emission (AIE) of organic fluorophores is of great importance for the design of new luminescent materials.[1,2] In AIE, the light-emitting properties of a molecule are greatly enhanced in the aggregate or solid state with respect to solution. This offers new possibilities in the field of organic light emitting devices (OLED) and optical sensors. One of the most widely accepted mechanisms is that intramolecular rotations promote the non-radiative decay in solution, while the restriction of intramolecular rotations (RIR) in the aggregate phase blocks the non-radiative decay. However, this explanation remains too general, and a detailed molecular mechanism, which would be very valuable for further design and application, is still missing.

Here we study AIE in diphenyl dibenzofulvene (DPDBF, Fig. 1), an electroluminescent hydrocarbon that has been used for the fabrication of OLEDs.[3] DPDBF is faintly fluorescent in acetonitrile solution. In water, it is insoluble and forms aggregates with a 35-fold increase in the fluorescence quantum yield. On the basis of the experimental results, RIR of the phenyl substituents was suggested to be responsible for the AIE. Using a Fermi golden rule type of approach, it has been suggested that the internal conversion rate of DPDBF in the solid state is determined by high frequency modes.[4] In solution, recent nonadiabatic molecular dynamics results obtained with the time-dependent Kohn–Sham (TD-KS) approach[5] suggest that two modes are responsible for the nonradiative decay: the low frequency twisting motion around the fulvene exocyclic double bond and a bond stretch in the dibenzofulvene (DBF) ring. While these studies give insight into some aspects of AIE in DPDBF, our aim is to provide a conceptual basis for the RIR model in this molecule, on the basis of high-level *ab initio* quantum-chemical calculations, together with a comprehensive picture of the photophysics of DPDBF in solution and the solid state.

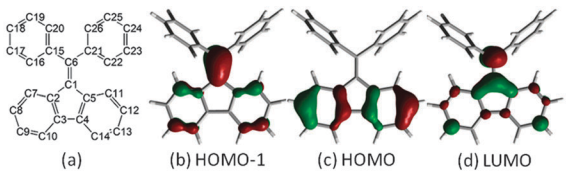

Fig. 1 (a) DPBDF structure with atom numbering, and (b)–(d) orbitals involved in the S_1 and S_2 excited states. S_1: HOMO → LUMO. S_2: HOMO − 1 → LUMO.

The photophysics of DPDBF has been modeled according to the MS-CASPT2//CASSCF approach, where critical points are optimized at the complete active space self-consistent field (CASSCF) level using Gaussian[6] and the energies are refined at the multi-state complete active space second order perturbation (MS-CASPT2) level with Molcas.[7] The structures are optimized in the gas phase, and the solvent effect (acetonitrile) is included by adding the CASSCF solvent-induced shift, calculated using the conductor polarizable continuum model (CPCM),[8] to the MS-CASPT2 gas phase energies (see computational details in the ESI†). In our discussion, we compare the experimental absorption and emission maxima with the computed vertical excitations at the ground and excited state minima, respectively, although these quantities do not correspond exactly to each other (see ESI† for details). In acetonitrile, the calculated vertical excitation energies are 3.12 eV and 4.01 eV for S_1 and S_2, respectively (see Table 1). S_2 absorption is predicted to be stronger than that of S_1. The maximum of the absorption band is predicted at 309 nm (vertical S_2 excitation wavelength), which is in good agreement with the experimental value of 322 nm.[3] In both states, the excitation involves promotion of an electron to an antibonding orbital along the C_1–C_6 bond (see Fig. 1). The excitation is almost completely confined within the dibenzofulvene (DBF) moiety because the phenyl substituents are not conjugated with the DBF ring due to steric hinderance. In consequence, the torsion of the phenyl groups

[a] *Key Laboratory of Cluster Science of Ministry of Education, School of Chemistry, Beijing Institute of Technology, 100081 Beijing, China*
[b] *Institut de Química Computacional i Catàlisi and Departament de Química, Universitat de Girona, Campus de Montilivi, 170071 Girona, Spain. E-mail: lluis.blancafort@udg.edu*

† Electronic supplementary information (ESI) available: Computational details and Cartesian coordinates of structures. See DOI: 10.1039/c3cc41730a

Table 1 Photophysical data for DPDBF in acetonitrile and in the solid, calculated at the MS-CASPT2//CASSCF(14,14)/ANO-S level of theory (structures optimized with CASSCF(12,12)/6-31G*). Energies given are relative to the ground state energy at the Franck–Condon structure

	Acetonitrile		Solid	
	E_{rel} [eV]	λ [nm]	E_{rel} [eV]	λ [nm]
S_1 vertical[a]	3.13 (0.002)[b]	397	3.17 (0.002)[b]	391
S_1 (E_{ad})[c]	2.59	478	3.11	401
S_1 emission[d]	1.46	846	2.20	563 (Expt. 460)[e]
S_2 vertical[a]	4.01 (0.007)[b]	309 (Expt. 322)[e]	4.05 (0.006)[b]	306 (Expt. 323)[e]
S_2 (E_{ad})[c]	3.52	352	3.79	328
S_2 emission[d]	3.04	408 (Expt. 441)[e]	3.54	350

[a] Vertical excitation energy. [b] Oscillator strength in brackets. [c] Adiabatic excitation energy. [d] Vertical emission from the minimum of the corresponding state. [e] Experimental values in brackets.

around the C_6–C_{15} and C_6–C_{21} bonds is only of secondary importance for the photophysics.

Experimentally, the photophysics of DPDBF was measured after excitation at 350 nm (3.54 eV).[3] This wavelength mainly populates the S_1 state. In our calculations, the origin of the S_2 state lies 3.52 eV above the ground state energy in the Franck–Condon geometry. Considering that the calculated S_2 vertical excitation is overestimated by 0.16 eV, we assume that the 350 nm excitation can also transfer a small fraction of population to the red wing of the S_2 state. The decay coordinate for S_1 and S_2 is dominated by two modes (see the bottom of Fig. 2a): a combined mode composed of the C_1–C_6 stretch, bond inversion in the fulvene ring and bond alternation in the DBF benzo rings, and the torsion of the phenyl substituents around the C_1–C_6 bond. Fig. 2 displays the C_1–C_6 bond length values, which are representative of the first mode, and the C_2–C_1–C_6–C_{15} dihedral angle φ for the torsion (see the detailed bond lengths in the ESI†). In our mechanism, the fraction of population transferred to S_2 relaxes to a minimum, **S_2-Min^{ac}**, where the torsion angle φ is 40° (the superscript **ac** stands for acetonitrile). The faint emission observed in experiments peaks at 441 nm (2.81 eV) and comes from this minimum, since the calculated emission of 3.04 eV (408 nm) is in good agreement with the experiment. Moreover, the S_2–S_1 energy gap in this structure is 0.62 eV, and there is a close-lying (S_2–S_1) intersection at approximately 3.8 eV above the **S_0-Min^{ac}** energy. Therefore, internal conversion to S_1 will compete with S_2 emission. The population that reaches S_1, either directly after excitation or *via* internal conversion from S_2, relaxes to the **S_1**-Min^{ac} minimum, which lies at 2.59 eV. However, the S_1 population does not contribute significantly to the fluorescence around 441 nm, since the calculated emission wavelength from this structure is 873 nm. Instead it decays further to the ground state through an (S_1–S_0) conical intersection (CI) seam. The minimum of the seam, **(S_1/S_0)-CI^{ac}**, is energetically accessible at 2.81 eV, since the vertical excitation energy is 3.54 eV. At this structure, the C_1–C_6 bond is completely twisted (φ = 90°). Our results also explain why the experimental excitation maximum (excitation wavelength that induces maximal emission) is found at 3.59 eV (345 nm), nearly 0.3 eV below the absorption maximum.[3] This excitation energy populates S_2, and fluorescence is favored because the (S_2–S_1) CI lies relatively higher in energy, at approximately 3.8 eV. In contrast, excitation energies higher than 3.59 eV facilitate the access to the S_1–S_2 intersection, transferring the population to the non-fluorescent S_1 state, whereas excitation energies lower than 3.59 eV favor direct population of S_1. Fluorescence is quenched in both cases.

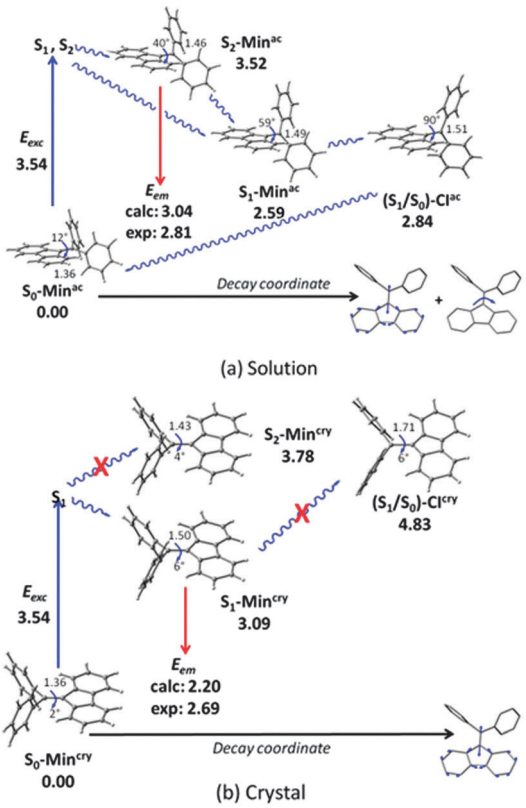

Fig. 2 Calculated mechanisms for the photophysics of DPDBF (a) in acetonitrile and (b) in the solid phase (crystal). Structural parameters: C_1–C_6 distance (representative of bond length changes in the DBF unit) and methylene torsion angle φ. Straight blue arrow: excitation. Straight red arrow: emission. Curled blue arrow: vibrational relaxation and internal conversion. Energies in eV.

The CI based model that explains AIE in DPDBF is illustrated in Fig. 3. The seam of intersection responsible for S_1 to S_0 decay in solution is similar to the one known for fulvene.[9] It lies along the bond stretch and torsion coordinates (Q_{CC} and Q_φ, respectively) and spans a series of CIs going from the highly twisted structure (φ = 90° and C_1–C_6 = 1.51 Å) to a planar structure (φ = 0°) with a highly stretched C_1–C_6 bond (1.80 Å). The seam has been mapped by optimizing several structures, with varying φ in steps of 10° (see ESI†). It spans an energy range from 2.81 eV at the minimum of the seam to 5.11 eV at the planar structure. The energetically accessible region of the seam (marked with a yellow line in Fig. 3), where the seam energy is lower than the excitation energy, contains geometries

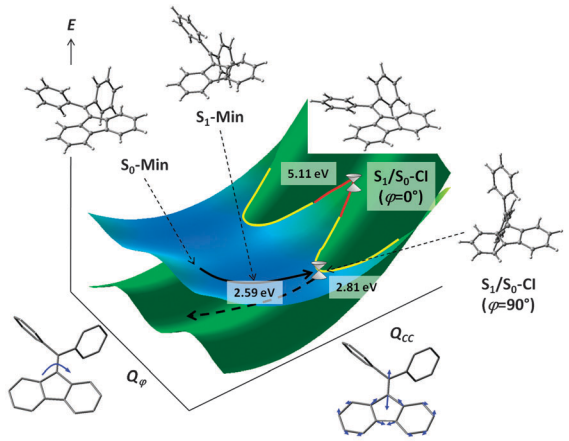

Fig. 3 Sketch of the S_1–S_0 CI seam for DBDBF in solution, along the bond stretch and torsion coordinates (Q_{CC} and Q_φ, respectively). The **ac** superscript has been dropped for clarity. Energies relative to the ground state energy of **S_0-Min^{ac}**.

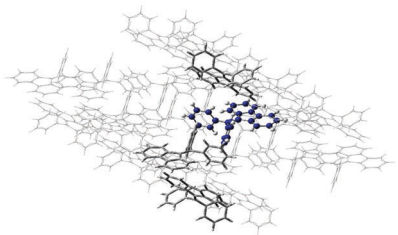

Fig. 4 Structure used for the excited state calculations in the crystal. The unit cell is formed by the four highlighted molecules. The ball-and-stick molecule is the one treated at the CASSCF level.

with a high twisting angle ($\varphi > 50^\circ$). In the solid, the twisting around the double bond is restricted because of the bulky phenyl substituents. Only the higher energy region of the seam, around planar geometries with a large C_1–C_6 stretch, will exist in the solid, explaining the increase in the fluorescence. The two coordinates that promote the decay agree with the ones derived from the TD-KS study,[5] and our results show that the nonradiative decay takes place at a seam of intersection. Time-resolved spectra for DPDBF would be interesting in this context to confirm that the excited state lifetime in solution corresponds to decay at a CI.

The calculations in the solid phase are carried out with a hybrid quantum mechanics:molecular mechanics approach within the ONIOM formalism.[10] Due to the bulky phenyl substituents, the DBF rings form non-parallel slabs (see Fig. 4). This disfavours exciton formation because the coupling between the DPDBF monomers is small, as proved by time-dependent density functional (TD-DFT) calculations described in the ESI.† Therefore, it is enough to treat a single DPDBF molecule at the quantum mechanical level, mechanically embedded in a crystal of 23 rigid molecules obtained from the crystallographic structure[11] and treated with the Universal Force Field.[12] The calculated vertical excitation spectrum of DPDBF in the solid (see Table 1) is similar to the one in solution, which is in agreement with the experimental data. However, the relaxation coordinate is restricted to changes in the bond lengths because the rotation of the bulky phenyl substituents is hindered (see Fig. 2b). As a consequence, the relative energy of the S_2 and S_1 minima in the solid, **S_2-Min^{cry}** and **S_1-Min^{cry}**, is increased compared to that in solution. These structures lie at 3.79 eV and 3.11 eV, respectively. The calculated vertical emission energy from these minima is 2.20 eV and 3.50 eV, respectively. In turn, the experimental emission maximum appears at 2.69 eV (460 nm). This indicates that, in contrast to the solution case, emission in the solid comes from the S_1 state. Moreover, decay to the ground state at the S_1–S_0 intersection seam is disfavored because the energy minimum of the seam in the crystal is a quasi-planar structure, **(S_1/S_0)-CI^{cry}** ($\varphi = 6^\circ$), with a high energy of 4.91 eV. This explains the increased emission intensity. The changes found for the emitting species in solution and in the solid (S_2 and S_1, respectively) show that the interplay between the two states is very important for the luminescence of DBF derivatives.

Our results have general importance for the understanding of AIE. Most theoretical approaches to AIE have been based on decay rate calculations based on a Fermi golden rule approach.[4,13–16] However, this approach should be used with care, at least in solution, because it is not valid to model the decay at a CI. In future work it will be important to determine if CIs play similar roles in the AIE of other organic luminophores, such as silole derivatives.[17]

We thank Denis Jacquemin (Université de Nantes, France) for advice on the TD-DFT calculations. This work was funded by the Spanish Ministerio de Ciencia e Innovación (MICINN) (CTQ2011-26573 and UNGI08-4E-003 from FEDER (European Fund for Regional Development)), and the Catalan Agència de Gestió d'Ajuts Universitaris i de Recerca (SGR0528) and Direcció General de la Recerca (Xarxa de Referència en Química Teòrica i Computacional de Catalunya). Q. Li acknowledges a Juan de la Cierva fellowship of the MICINN.

Notes and references

1 Y. Hong, J. W. Y. Lam and B. Z. Tang, *Chem. Commun.*, 2009, 4332–4353.
2 Y. Hong, J. W. Y. Lam and B. Z. Tang, *Chem. Soc. Rev.*, 2011, **40**, 5361–5388.
3 H. Tong, Y. Dong, Y. Hong, M. Haussler, J. W. Y. Lam, H. H. Y. Sung, X. Yu, J. Sun, I. D. Williams, H. S. Kwok and B. Z. Tang, *J. Phys. Chem. C*, 2007, **111**, 2287–2294.
4 M.-C. Li, M. Hayashi and S.-H. Lin, *J. Phys. Chem. A*, 2011, **115**, 14531–14538.
5 X. Gao, Q. Peng, Y. Niu, D. Wang and Z. Shuai, *Phys. Chem. Chem. Phys.*, 2012, **14**, 14207–14216.
6 M. J. Frisch, G. W. Trucks and H. B. Schlegel, *et al.*, Gaussian, Inc., Wallingford, CT, 2010.
7 F. Aquilante, L. De Vico and N. Ferre, *et al.*, *J. Comput. Chem.*, 2010, **31**, 224–247.
8 A. Klamt and G. Schuurmann, *J. Chem. Soc., Perkin Trans. 2*, 1993, 799–805.
9 F. Sicilia, M. J. Bearpark, L. Blancafort and M. A. Robb, *Theor. Chem. Acc.*, 2007, **118**, 241–251.
10 S. Dapprich, I. Komaromi, K. S. Byun, K. Morokuma and M. J. Frisch, *THEOCHEM*, 1999, **461**, 1–21.
11 H. Bock, K. Ruppert, E. Herdtweck and W. A. Herrmann, *Helv. Chim. Acta*, 1992, **75**, 1816–1824.
12 A. K. Rappe, C. J. Casewit, K. S. Colwell, W. A. Goddard and W. M. Skiff, *J. Am. Chem. Soc.*, 1992, **114**, 10024–10035.
13 S. W. Yin, Q. Peng, Z. Shuai, W. H. Fang, Y. H. Wang and Y. Luo, *Phys. Rev. B*, 2006, **73**, 205409.
14 Q. Peng, Y. Yi, Z. Shuai and J. Shao, *J. Am. Chem. Soc.*, 2007, **129**, 9333–9339.
15 Q. Wu, C. Deng, Q. Peng, Y. Niu and Z. Shuai, *J. Comput. Chem.*, 2012, **33**, 1862–1869.
16 Q. Wu, Q. Peng, Y. Niu, X. Gao and Z. Shuai, *J. Phys. Chem. A*, 2012, **116**, 3881–3888.
17 J. D. Luo, Z. L. Xie, J. W. Y. Lam, L. Cheng, H. Y. Chen, C. F. Qiu, H. S. Kwok, X. W. Zhan, Y. Q. Liu, D. B. Zhu and B. Z. Tang, *Chem. Commun.*, 2001, 1740–1741.

